FRACTURE RESISTANCE DEGRADATION OF HYBRID GLASS MATRIX COMPOSITE

I. Dlouhy[1]), Z. Chlup[1]), A. R. Boccaccini[2])
[1]) Institute of Physics of Materials, AS CR, 61662 Brno, Czech Republic
[2]) Department of Materials, Imperial College London, London SW72BP, UK
idlouhy@ipm.cz, chlup@ipm.cz, a.boccaccini@imperial.ac.uk

Abstract

The fracture behaviour of hybrid glass matrix composite before and after thermal ageing and/or thermal shock cycling in air has been analysed. Chevron notch technique was applied for fracture toughness determination. The K_{Ic} values were in the range 2.6-6.4 MPam$^{1/2}$ for the as received material and they were significantly reduced by thermal loading. The K_{Ic} values dropped to 0.4 MPam$^{1/2}$ for ageing at 700 °C for 24 h due to fibre oxidation and porosity formation in the matrix as a result of softening of the glass. The K_{Ic} values decreased to 1.3 MPam$^{1/2}$ for the 24 thermal shock cycles from 500°C and/or to 1.1 MPam$^{1/2}$ for 50 cycles from 600°C. The damage in the samples due to thermal shock cycling was explained by fibre oxidation and porosity formation, as in case of thermal ageing, and, in addition, by superposed residual thermal stresses in the matrix produced by repeated thermal shocks.

Introduction

Hybrid composites are created incorporating simultaneously fibres, particles and/or whiskers as reinforcing elements. In hybrid glass matrix composites, the fibres (e.g. chopped or continuous carbon or SiC fibres) are used to impart fracture resistance by exploiting well-known fracture mechanisms such as fibre pullout and crack deflection. The particulate phase is used to improve other engineering properties relevant for the intended application of the materials, such as thermal shock resistance, wear resistance or impact strength. The few hybrid glass and glass-ceramic matrix composites described in the literature include: barium magnesium aluminosilicate glass-ceramic composites containing both SiC-Nicalon® fibres and SiC whiskers [1,2], cordierite glass-ceramic matrix composites with SiC monofilament and SiC whiskers [3], borosilicate glass containing SiC-Nicalon® fibres, carbon fibres and various ceramic particle fillers (alumina, zirconia or carbon) [4] and aluminosilicate glass containing SiC-Nicalon® fibres and SiC particles [5]. Recently, fused silica matrix composites containing Si_3N_4 particles and chopped carbon fibres have been developed [6].

In brittle matrix composites reinforced by continuous ceramic fibres, the favourable fracture behaviour is provided by the presence of weak fibre/matrix interfaces, which lead to the fibre pullout effect [7]. The thermal stability and high temperature mechanical properties of silicate matrix composites reinforced by carbon and SiC based fibres in oxidising environments have been investigated quite extensively in the past [8,9]. A common result of investigations conducted at temperatures in the range 500-700 °C is that there is a decrease of tensile and flexural strength of the composites. It has been shown that this is the consequence of oxidation of the fibres, in case of carbon fibre reinforced composites, or of degradation of the fibre/matrix interphase, which is in fact a carbon-rich nanometric interfacial layer, in SiC fibre reinforced composites [8,9]. Since very little research has been conducted in the area of

hybrid glass matrix composites so far, there is need for investigations, in particular regarding the fracture behaviour of the material after thermal loading in oxidising atmospheres.

In the present investigation, the chevron notch specimen technique was used to detect the degradation of the flaw resistance and fracture toughness of hybrid glass matrix composite after thermal ageing and thermal shock cycling in air. Another objective of the article was to examine the applicability of the chevron-notch technique to monitor possible changes in the fracture toughness due to microstructural damage in this class of composite materials.

Experimental procedures

The material investigated was a hybrid glass matrix composite supplied by Schott Glas (Mainz, Germany). The composite contained short carbon fibres (24 wt%) as well as ZrO_2 particles (30 wt%) dispersed in a borosilicate glass (DURAN®) matrix. The density of the composites was 2.62 g/cm^3. Details of the fabrication procedure are given in the literature [4].

Rectangular test bars of nominal dimensions 4 mm x 3 mm x 50 mm were cut from the plates. Thermal aging for 24 h was carried out in air using an electric furnace at temperatures of 500, 600 and 700 °C. Another set of specimens was exposed to repeated thermal shocks produced by quenching samples from 500 °C and/or 600 °C into a water bath kept at room temperature. After each quench, the samples were heated again for 15 minutes. Specimens were further characterised after 5, 10, 20, and 24 and/or 50 cycles. The temperatures chosen for this study cover the ranges at which the composites are likely to find applications [10].

The microstructures of the both as received and thermally loaded samples were observed by scanning electron microscopy using both secondary electron and backscattered electron image modes. A SEM micrograph showing the microstructure of an as-received sample is shown in Fig. 1a. Fig. 1b shows the same area in backscattered electrons revealing (due to different phase contrast) the distribution of ZrO_2 particles (white phase) in the glass matrix.

The fracture toughness was characterised using the chevron-notched specimen technique. Chevron notches with angles of 90° were cut at distances of about 15-20 mm in each test bar using a thin (0.15 mm) diamond wheel. Because the span of the three-point bend test was 16 mm, several notches were introduced in each bar (of 50 mm length). Each bar was then placed in the three-point bend fixture and loaded up to fracture initiation. A constant crosshead speed of 0.01 mm/min was employed for loading. The tests were carried out at room temperature in normal atmosphere.

Graphs of load vs. time were recorded and the maximum force was determined from each trace. The fracture toughness value, K_{Ic}, was calculated from the maximum load (F_{max}) and the corresponding minimum value of geometrical compliance function (Y^*_{min}), The calculation procedure used for the purposes of this investigation has been described in detail elsewhere [11]. The chevron-notch depth a_0, needed for determining Y^*_{min}, was measured after testing from optical micrographs of fractured specimens. Additionally, the acoustic emission technique was used during the test. Traces of cumulative number of acoustic emission (AE) events were obtained in the same time scale as the load vs. time plots. This technique allows for an accurate detection of the onset of microcracking at the chevron notch tip, which occurs when a sharp increase in the number of AE events is observed.

Fracture surfaces of selected broken samples both in as-received condition and after thermal ageing were observed by optical stereomicroscopy and SEM. A more comprehensive description of other methods applied to characterised the hybrid composites has been presented elsewhere [11].

Results

As-received material

The as received material exhibits K_{Ic} values in the range 2.6-6.4 MPam$^{1/2}$. These values are higher than K_{Ic} values quoted for unreinforced borosilicate glass (0.77 MPam$^{1/2}$ [12]) and for Al_2O_3 platelet (30 vol%) reinforced borosilicate glass composites (1.92 MPam$^{1/2}$ [13]). The values are similar to data reported in the literature for hybrid glass matrix composites reinforced by unidirectional SiC fibres and SiC whiskers [2] and for silica matrix composites containing Si_3N_4 particles and C fibres [6], but they are much lower than K_{Ic} data of composites reinforced by 40 vol % of unidirectional SiC fibres (19-26 MPam$^{1/2}$ [12]). The scatter of data in the present composites was however found to be extremely high [11]. This is connected with different orientations of chopped fibre bundles below the chevron notch tip.
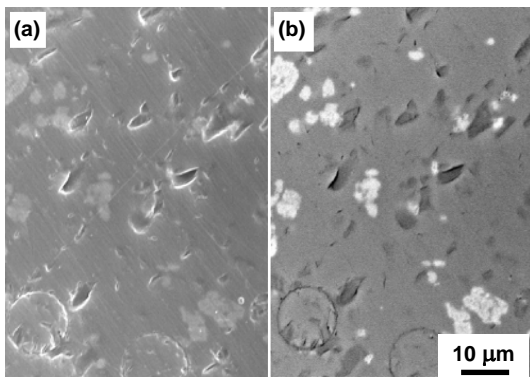
FIGURE 1. Polished section showing (a) fibres and ZrO_2 particles; (b) the same region in back scattered electrons mode.
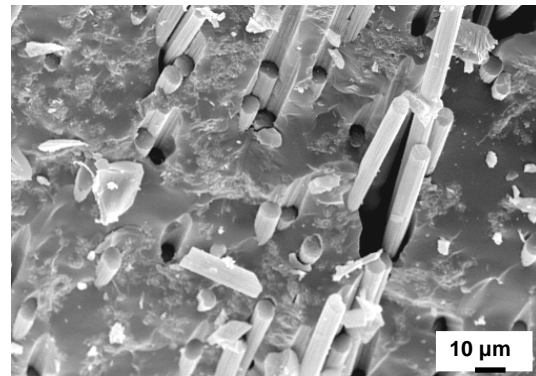
FIGURE 2. Typical fracture surface morphology of a broken test specimen (as received state), showing fibre pull-out.

The fracture surface (Fig. 2) exhibits the fiber pull-out typical of "quasi-ductile" glass matrix composite materials. However, inspection of the fracture surfaces revealed that the average pull-out lengths are not uniform across the composite section but depend on the relative orientation of the fibre bundles and the fracture propagation plane. Areas exhibiting fewer fibres are observed when these were oriented parallel to the fracture surface. This behaviour explains qualitatively the lower K_{Ic} values determined in this material in comparison to unidirectional fibre reinforced composites, as mentioned above, where all fibres contribute equally to toughening by the pull-out mechanism [10,12].

Thermally aged material

The fracture resistance of the composite substantially decreased due to microstructural changes induced by thermal ageing. The change of fracture behaviour can be appreciated from the load-deflection traces. The traces for the as received composite and for the material after thermal ageing (Fig. 3) show a significant decrease in the maximum value of the fracture load for similar chevron notch and specimen geometry. In addition to these characteristics, directly related to a decrease in K_{Ic} values, a change in the slope of the linear part of the traces can also be seen in Fig. 3. The decrease in slope with increasing exposure temperature corresponds to a decrease of specimen compliance that can be explained by poorer fibre/matrix interfacial bond and, for the most severe thermal ageing, by matrix

damage due to softening and porosity formation as a result of carbon fibre oxidation. A decrease in Young's modulus is a direct consequence of this type of microstructural damage.

The fracture toughness values determined by the chevron notched specimen technique are strongly dependent on the ageing condition, as shown in Fig. 4.
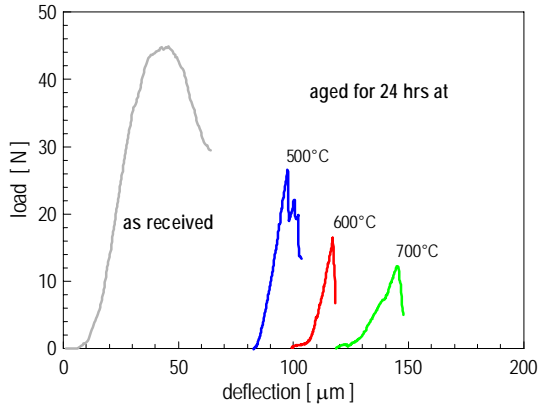
FIGURE 3. Typical load-displacement plots obtained in chevron-notch tests for as-received condition and after thermal ageing.
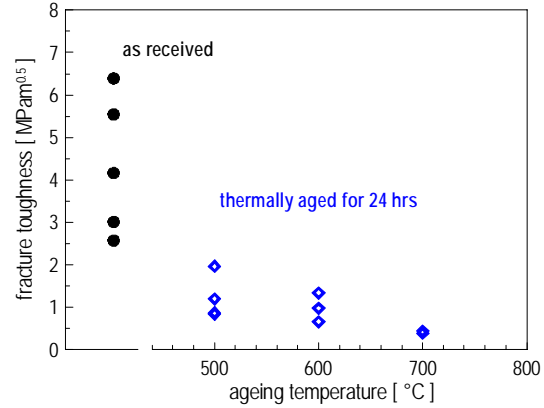
FIGURE 4. The effect of ageing conditions on fracture toughness of the hybrid composite.

The poorest mechanical response of the samples aged for 24 h at 700 °C is evident from comparison of data in Fig. 4. It should be noted that microstructural damage accompanying the thermal ageing has produced localised macroscopic shape and volume changes in the samples, with the extent of this damage depending on fiber bundle orientation. This was most evident for the above mentioned condition of ageing (24 hrs at 700 °C) and it is most probably related to softening of the glass matrix, as discussed below. The measured fracture toughness value for this composite was $K_{Ic} = 0.4$ MPam$^{1/2}$.
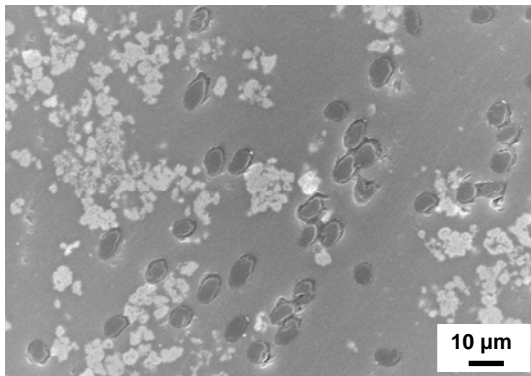
FIGURE 5. SEM micrograph of a polished section showing microstructure after ageing for 24 h at 500 °C.
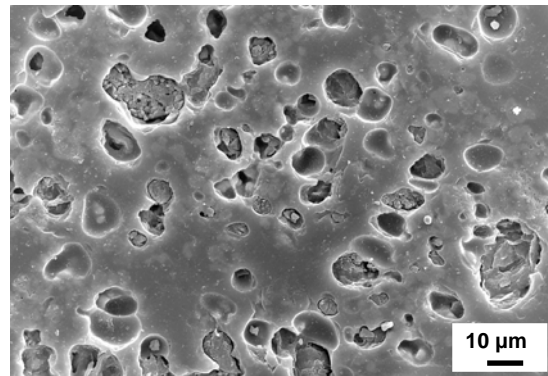
FIGURE 6. SEM micrograph of a polished section showing microstructural degradation after ageing for 24 h at 700°C

The microstructures of thermally aged samples (areas of composite sections oriented perpendicularly to the fibres) are shown in Figs. 5 and 6 for the ageing conditions 500°C/24h

and 700°C /24h, respectively. It is evident that at 500 °C the carbon fibres remain in the composite, however the begin of fibre oxidation leads to the loss of contact between fibre and matrix (Fig. 5). The image also shows that there is no development of porosity and the overall microstructural damage is limited. Microstructural damage is severe in the composite aged for 24 h at 700 °C (Fig. 6). Comparing to as-received specimens (Fig. 1), high porosity in the aged samples is evident, which can be explained by the carbon fibres decomposition due to oxidation effects. Moreover, softening of the glass matrix at elevated temperature may have contributed to the formation of cavities.

Material exposed to repeated thermal shocks

The investigation of load-deflection traces provided very valuable information for the assessment of damage development in thermally shocked samples. For repeated thermal shocks from 500°C, the typical curves are shown in Fig. 7. Similarly as in case of thermal ageing, the load-deflection curves and K_{Ic} values are strongly affected by the orientation of fibre bundles with respect to the chevron notch plane. In case of parallel orientation, the remarkable drop of fracture resistance is associated with the significant change of the load-deflection trace as it can be seen, as example, comparing the curves for specimens after 10 thermal shock cycles in Fig. 7: specimen 2_3 displayed nearly parallel orientation of fibers and fracture plane, while specimen 2_1 displayed random fibres orientations.

After the first five thermal shock cycles the fracture behaviour is very similar to that of as received composites (compare the corresponding curves in Figs. 3 and 7). For higher number of thermal shock cycles two typical features arise on the load deflection traces. The first one is a marked pop-in behaviour at loads of about 10 N (marked by circles in Fig. 7). The second phenomenon observed is increasing specimen deflection at fracture (maximum) load, as evident when comparing the curves for 10 and 24 cycles in Fig. 7. This can be caused by the change of crack tip behaviour affected by damage development at the matrix/fibre interfaces.
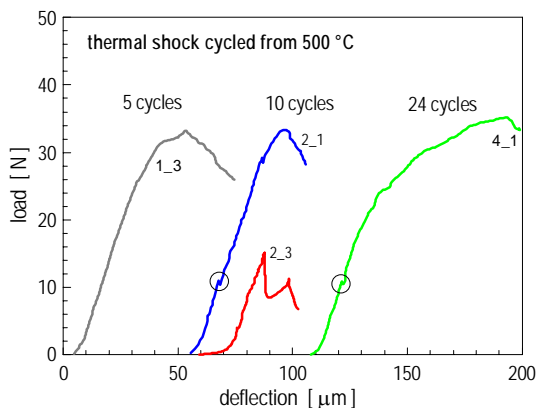
FIGURE 7. Typical load-displacement plots obtained in chevron-notch tests for different number of repeated thermal shocks
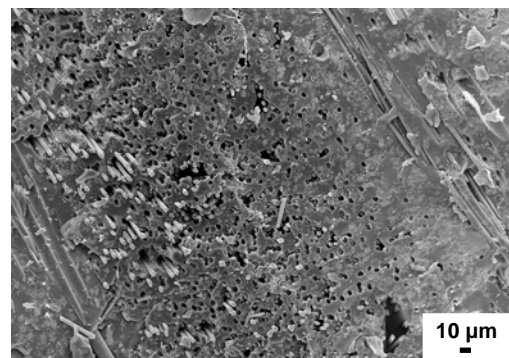
FIGURE 8. SEM micrograph showing a typical fracture surface of the composite after 20 thermal shock cycles

The fracture toughness values determined by the chevron notched specimen technique are strongly dependent on the condition of thermal shock, in particular for the first ten thermal shock cycles, as shown in Fig. 9 for shock cycling from 500°C and in Fig. 10 for shock cycling from 600°C. In these figures, the fracture toughness values are represented by two

kinds of points. Filled triangles represent the values obtained in those specimens where fibers are randomly oriented in relation to the chevron notch plane. The empty triangles are for the fracture toughness values representing data from specimens with fibre bundles parallel to the chevron notch plane. It is clearly evident how the fracture resistance and thus fracture toughness strongly depends on the fibre bundle orientation.

Fig. 8 shows a SEM micrograph of the fracture surface of a sample thermally shocked for 20 cycles. Very limited pull-out is detected in this sample, which is similar to observations on samples thermally aged at 500 °C for 24 hours, as discussed above.

In Fig. 9, also data of the as received material (filled circles) and material aged at 500 °C for 24 hrs (empty rhombi) are shown for comparison. It is seen that the most significant part of composite damage occurred during the first 10 thermal shock cycles. However, the total exposition time at 500 °C during this treatment was comparably shorter than in case of thermal ageing analysed in previous chapter. The more extensive and rapid damage during thermal shock cycling is thus ascribed to the quenching effect, in particular to the effect of cumulative thermal stresses produced during repeated thermal shocks. For the thermal cycling from 600°C similar findings have been obtained.
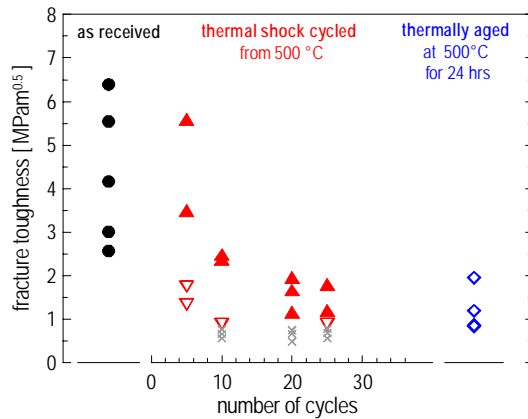
FIGURE 9. The effect of thermal shock cycling from 500°C on fracture toughness
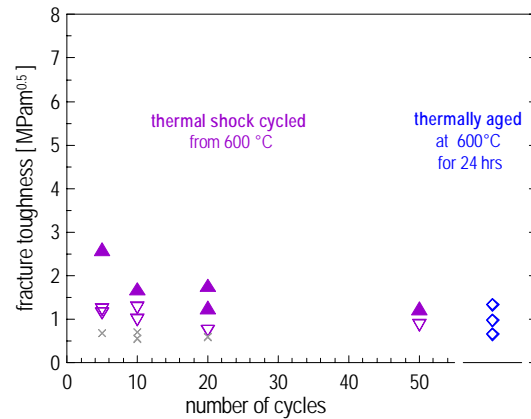
FIGURE 10. The effect of thermal shock cycling from 600°C on fracture toughness

Discussion

The fracture toughness values of the hybrid composites investigated are in the range 2.6-6.4 $MPam^{1/2}$ and they exhibit an extremely large scatter. This was associated with different orientations of short fibre bundles in relation to the chevron notch plane as discussed in detail on the basis of microstructural and fracture surface observations. In general, the as-received material exhibit relatively high K_{Ic} values, in comparison with other hybrid glass matrix composites [2,6,13], which suggests that an effective part of the toughening effect may be provided by the zirconia particles added. The addition of tetragonal zirconia particles to glass matrices should contribute to toughening by the tetragonal-to-monoclinic transformation mechanism. However in the present composite a monoclinic zirconia particulate phase was added, thus ruling out transformation toughening. In fact the presence of a particulate zirconia phase dispersed in a brittle matrix may further contribute to toughening and strengthening by other mechanisms, mainly by crack deflection and by residual thermal stresses [15]. In the present composites, a favourable residual thermal stress field (hoop

compressive stresses in the matrix) should develop upon cooling from the fabrication temperature as a result of the thermal expansion mismatch between the zirconia particles (10.3 10^{-6} 1/°C [16]) and the borosilicate glass matrix (3.25 10^{-6} 1/°C [12]). However, the relative contribution to toughening due to the fibre pull-out mechanism and to zirconia particle related mechanisms cannot be quantitatively determined from the results obtained in this study. In general, however, fibre pull-out is thought to be the dominant and more effective toughening mechanism in these hybrid composites [11].

For the most severe thermal ageing conditions (700 °C, 24 h, Fig. 4), the K_{Ic} values dropped to 0.4 MPam$^{1/2}$. This value is even lower than K_{Ic} of monolithic borosilicate glass (0.77 MPa m$^{1/2}$ [13]), which can be explained by the very high porosity developed in the aged sample as consequence of carbon fibre oxidation. Thus, for the conditions of thermal ageing investigated here, degradation of carbon fibres due to oxidation occurred, this being more severe with increasing temperature, and therefore the apparent fracture toughness and flaw tolerant resistance of the composites decreased. For the highest temperature tested (700 °C), enhanced porosity formation in the matrix was detected, which is thought to be the result of softening of the glass. Indeed the aging temperature (700 °C) was well above the transformation temperature of the borosilicate glass matrix used (T_g = 525 °C for borosilicate DURAN® glass [10]). It seems that oxidation of the carbon fibres starts at 500 °C, leading to degradation of the fibre – matrix interface. As shown in Fig. 5 for a polished sample, the interface boundary between the glass matrix and fibres appears to be degraded comparing to the initial state (Fig. 1). The combination of matrix and matrix-fibre interface degradation and the damage to the boundary region between neighbouring fibre bundles, as detected by scanning electron microscopy observations (Figs. 5 and 6), supplied a more favourable condition for fracture initiation and this resulted in a decrease of both K_{Ic} values and the data scatter in thermally aged materials.

A similar detrimental effect on K_{Ic} values was measured in samples after repeated thermal shocks from 500 °C and 600°C. K_{Ic} dropped to 1.3 MPam$^{1/2}$ for the maximum number of thermal shocks applied (Fig. 9) and to 1.1 MPam$^{1/2}$ (Fig. 10). The figures also indicates that the K_{Ic} values of shocked samples lie between those of as received samples and those of specimens thermally aged at 500 °C for 24 hours. This is related to the shorter exposure time at high temperature in the thermally shocked samples in comparison to the aged samples.

The actual contribution of the thermal shocks to composite degradation is hard to quantify and the samples have undergo degradation also during the holding time at temperature. There is an important effect that has been detected however when comparing the load-deflection traces of specimens thermally aged (Fig. 3, see the curve for 500 °C) and specimens after thermal shock cycling (Fig. 7, curves for 10 and 24 cycles). Occurrence of pop-in effect at loads of about 10 N appeared to be typical for specimens after thermal shock treatment. An attempt has been made to estimate the stress intensity factor (fracture toughness value) corresponding to this level of load for particular specimens. This is possible assuming that the dependence of the geometrical function on crack length is known for the particular chevron notch depth. The values obtained are represented by crosses in Fig. 7; they correspond well to the fracture toughness of the borosilicate glass matrix used in the composite (0.7 MPam$^{1/2}$ [12]). One possible explanation is that whereas high temperature exposition (ageing) leads to carbon fiber and fiber matrix interface degradation, the thermal shock loading causes additional damage to the matrix. This can be due to residual thermal stresses developed in the matrix after increasing number of thermal shocks, which causes premature matrix microcracking at the chevron notch tip in the early stages of specimen loading. This indicates that cumulative degradation of the composite due to increasing number of thermal shocks is more detrimental compared to simple thermal exposition (ageing) at the same temperature.

Conclusions

The fracture behaviour of hybrid glass matrix composite samples before and after thermal ageing and/or thermal shock cycling in air has been analysed and evaluated for the first time. The fracture toughness values measured were in the range 2.6-6.4 MPam$^{1/2}$ for the as received material and they were significantly reduced by thermal ageing and thermal shock treatments. The K_{Ic} values dropped to 0.4 MPam$^{1/2}$ for ageing at 700 °C for 24 h due to fibre oxidation and porosity formation in the matrix as a result of softening of the glass. The K_{Ic} values decreased to 1.3 MPam$^{1/2}$ for the maximum number of thermal shock cycles from 500 °C (24 cycles) and to 1.1 for the maximum number of thermal shock cycles from 600°C (50 cycles). The damage in the samples due to thermal shock is based on fibre oxidation and porosity formation, as in case of thermal ageing, and, in addition, due to superposed residual thermal stresses in the matrix produced by repeated thermal shocks.

Acknowledgements

References

1. Chawla, N., Chawla, K.K., Koopman, M., Patel, B., Coffin, C., Eldridge, J. I., *Comp. Sci. Technol.*, **61**, 1923-1930, 2001.

2. Lewinshon, L.A., *J. Mat. Sci. Lett.*, **12**, 1478-1480, 1993.

3. Haug, S. B., Dharani, L. R., Carroll, D. R., *Appl. Comp. Mater.*, **1**, 177-181, 1994.

4. Reinicke, R., Friedrich, K., Beier, W., Liebald, R., *Wear,* **225-229**, 1315-1321, 1999.

5. Gadkaree, K.P., *J. Mat. Sci.,* **27**, 3827-3834, 1992.

6. Jia, D.C., Zhou, Y., Lei, T.C., *J. Europ. Ceram. Soc.*, **23**, 801-808, 2003.

7. Evans, A.G., Zok, F.W., *Review. J. Mat. Sci.*, **29**, 3857-3896, 1994.

8. Sutherland, S., Plucknett, K.P., and Lewis, M.H., *Comp. Eng.*, **5**, 1367-1378, 1995.

9. Prewo, K.M., Batt, J.A., *J. Mat. Sci.*, **23**, 523-527 (1988).

10. Boccaccini, A.R., Pearce, D.H., Janczak, J., Beier, W., and Ponton, C.B., *Mat. Sci. Technol.*, *13*, 852-859, 1997.

11. Dlouhy, I., Chlup, Z., Atiq, S., Boccaccini, A.R., *Composites Part A*, 34, 1177–1185, 2003

12. Dlouhy, I., Boccaccini, A.R., *Scripta Mat.*, **44** (3), 531-537, 2001.

13. Boccaccini, A.R., Winkler, V., *Composites A*, **33**, 125-13, 2002.

14. Boccaccini, A.R., Strutt, A.J., Vecchio, K.S., Mendoza, D., Chawla, K.K., Ponton, C.B., and Pearce, D.H., *Composites A*, **29**, (11), 1343-1352, 1998.

15. Sarno, R. D., and Tomozawa, M., *J. Mat. Sci.*; **30**, 4380-4388, 1995.

16. Green, D.J., *An Introduction to the Mechanical Properties of Ceramics,* Cambridge University Press, Cambridge, UK, 1998.